

RHEOLOGICAL CHARACTERIZATION OF THERMOPLASTIC SUSPENSIONS FOR MICRO-FABRICATION BY CO-EXTRUSION OF PIEZOELECTRIC COMPOSITES (PZT) IN LOW DENSITY POLYETHYLENE (LDPE)

V. L. Bueno^{(1),(2)}, M. R. Ismael⁽²⁾, F. J. Clemens⁽²⁾, T. Graule⁽²⁾ and C. P. Bergmann⁽¹⁾

(1) Ceramics Materials Laboratory, LACER, Department of Materials, Federal University of Rio Grande do Sul, Brazil.

(2) EMPA, Swiss Federal Laboratories for Materials Testing and Research, Laboratory for High Performance Ceramics, Switzerland.

Correspondent author: viviane.bueno@ufrgs.br

ABSTRACT

The process of micro-fabrication by co-extrusion (MFCX) was investigated in order to obtain composite structures of lead zirconate titanate (PZT) in-situ. The principle of this technique is to assemble a preform, composed of two or more ceramic polymer compounds (feedstocks) in the desired cross section of the final product, which is obtained by flowing through a capillary die. The different compounds must have the same rheological behaviour so that they can flow together, making the preform suffer only a reduction in diameter by passing through the capillary. The main material used in this work was a feedstock consisting of PZT powder and low density polyethylene (LDPE), which provides the viscoelastic behaviour above the melting point for the mixture and improves its mechanical strength and the handling of the composites when at green state. To obtain the later 1-3 structure after sintering a second feedstock, either carbon black (CB) or microcrystalline cellulose (MCC) can be used which left a space that can be fulfilled with polymer in a final step. To investigate the influence of the wall slip effect on the shape stability during MFCX, cylindrical preforms with a cross section of half-moon have been used. One of the halves was a standard composition of 58 vol. % PZT + 42 vol. % LDPE, the other part consist feedstock composition either 25 vol. % CB + 75 vol. % LDPE or 41 vol. % MCC + 59 vol. % LDPE. The shape and the interface stability of obtained internal structure inside se filaments were characterized by image analysis. It was found that mixtures of MCC/LDPE and CB/LDPE were able to flow concurrently only by including the wall slip into the viscosity of the materials. After changing the parameters of the process, a good match between perform and coextruded structures occurred.

Key-words: co-extrusion; piezoelectric composites; wall slip effect; rheology.

1. INTRODUCTION

Since the piezoelectric effect was discovered in 1881 [1, 2], the applications and study about this phenomenon has been increasing. Lead zirconate titanate [$\text{Pb}(\text{Zr}_x\text{Ti}_{1-x})\text{O}_3$; PZT] materials exhibit that effect being suitable, when in the fibre form, for an incorporation into composite structures used as actuator and sensor. Fine-scale diameter fibres are desirable for such composites due to the fact that they can be operated with increased magnification and actuation [3]. Different methods for forming fine-scale piezoelectric fibres have been developed such as thermoplastic extrusion [4, 5], viscous solution spinning process – VSSP [6, 7], sol-gel [8] and electrophoretic deposition [8]. The difficulty of handling these micro-fine fibres to achieve 1-3 composite structures required the development of a manufacturing process called micro-fabrication by co-extrusion (MFCX) [9]. With this processing route not only 1-3 composites were fibres are aligned within a polymeric matrix are easy to process. Also 3-1 (honeycomb structure) and 2-2 (laminare structures) can be builded up [10, 11, 12, 13, 14, 15, 16]. The MFCX process is comprised of three main steps: preform formation, extrusion, and final burnout of organic binder components and sintering of the composite structure (Figure 1). The detailed overview about this method can be found on reference [10].

To obtain a successful MFCX, the materials have to be capable of maintaining the preform geometry after the reduction of its dimensions without axial, cross-sectional deformations or mixing at the interface of the different materials. In view of that, this process requires a detailed rheological characterization of the ceramic-binder compounds (feedstocks) being co-extruded. Instabilities due to differences in the flow behaviour of the feedstocks may lead to instabilities such as encapsulation phenomena [10, 13, 18] caused mainly by the tendency of the less viscous material to migrate towards the region of highest shear, since this minimises energy dissipation. Interface instabilities might also occur due to discrepancies in the rheology of the compositions [19]. However, in polymer-ceramics based systems, these instabilities have not been widely reported.

In all ceramic MFCX literature mainly the viscosity between the different feedstocks is adjusted in a certain shear rate area. This might be sufficient for simple structures, but if different feedstocks will have be contact to the wall of the die, it is obvious that wall slip effect as to be taken into account too [20]. Near the wall, the fluid

experiences high shear gradients and the particles tend to migrate towards the centre of the die. Considering that the centre of a single particle cannot approach the solid wall to a distance less than the effective radius of the particle, the concentration of the suspension near the rigid boundary is decreased, creating a thin binder layer in which the viscosity is obviously smaller than the global viscosity of the paste achieving a different velocity (v_{slip}) increasing the flow rate of the process [22]. The analysis of the flow curves is simplified when they are plotted in a diagram relating the shear stress at the wall versus the apparent shear rate. The material tested has to agree with four hypotheses to generate only one flow curve, independent of the dimension of the die and the material which it is made from, this curve is called “master curve”. The conditions are: (i) the material is incompressible; (ii) its behaviour is time independent; (iii) the experiments are isothermal; (iv) the material sticks at the wall [26]. The results obtained led to separate curves. Hypothesis i, ii and iii were satisfied, so, there was a breakdown of (iv), i.e. it could prove the existence of slip at the wall.

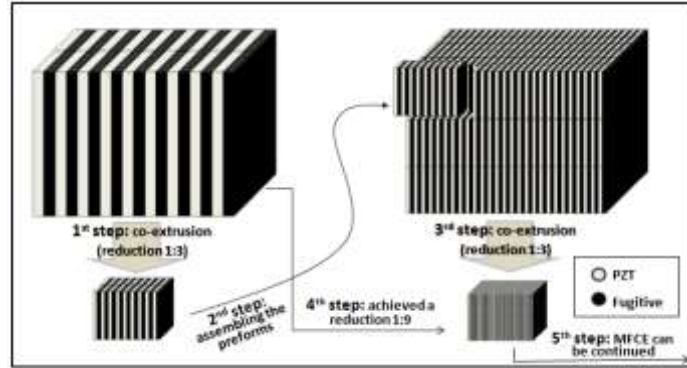


Figure 1. Schematic representation of MFCX process [14].

As for the slip velocity characterisation, one can easily make use of the well-known method proposed by Mooney [21]. Normally, the capillary rheometer calculates the shear rate from the volume flow rate (Q) and the dimensions of the capillary (length – L and diameter – D) by assuming that the velocity of the extrudate at the die wall is zero. This calculation is invalid if the velocity at the wall is not zero, but with an appropriate choice of dies, several sets of results can be combined to provide a correction [20]. This gives a value for wall slip velocity by Mooney’s method [21]. The presence of a boundary layer of dispersion medium of small thickness alters the structure of the stream. The increase in fluidity in the boundary layer in comparison with the fluidity in the volume leads to an increase in the flow rate [22]. The experimentally observed flow rate, Q_{obs} , may be intuitively considered to be composed of two nominally separated flow contributions:

$$Q_{obs} = Q_{bulk} + Q_{slip} \tag{Equation 1}$$

The first term on the right hand side is the intrinsic internal (developed) shear flow rate, and the second term is the separate contribution provided entirely by the wall slip at the wall. Eq. 1 may be converted to Eq. 2:

$$\frac{32Q}{\pi D^3} = \frac{4}{\tau_w^3} \int_0^{\tau_w} \tau^2 \gamma d\tau + \frac{8v_s}{D}, \quad v_{obs} = v_{bulk} + v_{slip} \tag{Equation 2}$$

where v_{obs} , v_{bulk} and v_{slip} are the mean observed, bulk (internally derived) and wall slip velocities, respectively.

The first terms on the right hand side of the equation describes the part of the nominal Newtonian shear rate that depends only upon the shear stress at the wall, as oppose to the capillary tube diameter. Mooney proposed an expression for $f(\tau_w)$ which depends upon the wall shear stress only:

$$V_s = f(\tau_w) = \alpha \tau_w \tag{Equation 3}$$

where α is the slip coefficient and hence:

$$\frac{32Q}{\pi D^3} = \frac{4}{\tau_w^3} \int_0^{\tau_w} \tau^2 \gamma d\tau + (8\alpha \tau_w) \frac{1}{D} \tag{Equation 4}$$

The partial derivative of Eq. 4 with respect to $1/D$ with τ_w fixed, results in the expression for the slip velocity from which the wall slip velocity can easily be determined with flow curves obtained by several capillary dies of

different diameters [22]. Once the slip velocity is determined as a function of the wall shear stress, the viscosity as a function of shear rate can be determined. The true shear rate at the wall can be obtained by:

$$\dot{\gamma}_T = \frac{4(Q - \pi r^2 v_s)}{\pi r^3} = \dot{\gamma}_a - \frac{4}{r} v_s \quad (\text{Equation 5})$$

where the usual apparent shear rate, $\dot{\gamma}_a$, is defined by:

$$\dot{\gamma}_a = \frac{4Q}{\pi r^3} \quad (\text{Equation 6})$$

It is clear that if the apparent shear rate is plotted against $1/r$, for a certain shear stress, than the intercept of this graph on the y-axis gives $\dot{\gamma}_T$ and the slope is $4v_s$. This only works if the shear stress is not a function of r , and this can be achieved by ensuring that the ratio L/R , where L is the die length, is kept constant. Mooney's method requires the use of, at least, three dies with different diameters to create the linear graph to get the true shear rate and slip velocity values. Even with the same L/D ratio, the ratio between the surface of the wall and the volume of the capillary decreases when the diameter of the die increases. Thus, different pressure drops will be verified for different dies during the extrusion process due to the surface of the wall, if the wall slip effect occurs. The range of apparent shear rates should be similar for all the tests. Since the shear rate is plotted against $1/r$ on linear axis, the die diameters should be chosen to give a good spread when their reciprocals are taken [22].

2. EXPERIMENTAL METHODS

2.1 Preform assembling

A description of the raw materials used in this work is listed in Table 1. Microcrystalline cellulose (MCC) was employed as an option to avoid the inorganic impurities left over on the surface of the co-extruded fibres after debinding when CB was used as auxiliary material [23, 24]. The thermoplastic binder was chosen based on previous work [25]. The density values were obtained using a helium pycnometer (Micromeritics, AccuPyc 1330). The specific surface area (SSA) was determined from a five point N_2 adsorption isotherm obtained from BET measurements (Beckman-Coulter SA3100, Beckman-Coulter, USA). To stabilize the mixture against agglomeration and promote proper binder wetting on the PZT ceramic, stearic acid (Fluka AG) was used as a surfactant. Further details concerning this coating procedure have been described previously [25].

Table 1. Raw materials used for processing.

Raw - material	Density (g/cm ³)	Degradation Temperature (°C)	SSA (m ² /g)	Supplier
PZT	7.86 ± 0.02		1.96 ± 0.05	CeramTec AG, Germany
CB	1.90 ± 0.08	350	30.00 ± 0.03	Cabot Corporation, USA
MCC	1.58 ± 0.06	220	0.95 ± 0.05	Sigma Aldrich, Germany
LDPE	0.92 ± 0.05	108		Lacqtene, Elf Atochem S.A., Switzerland

The compositions of the suspensions *a* and *b* (**¡Error! No se encuentra el origen de la referencia.**) were chosen based on previous work [10, 23]. An amount of 0.18 wt. % of laccaic acid (Sigma Aldrich) was used as a dye in the suspension *c* to allow the visualization of the interface between PZT and MCC after co-extrusion. The composition *d* has become necessary in order to obtain the half-moon geometry. Each preform was assembled using two suspensions (Figure 2).

Table 2 Properties and parameters of the suspensions used in the co-extrusion investigations.

Suspension	58 vol. % PZT (a)	25 vol. % CB (b)	41 vol. % MCC (c)	48 vol. % PZT (d)
Amount of powder (g)	205.90	22.94	31.29	170.40
Amount of LDPE (g)	18.66	33.33	26.22	23.11
Amount of dye (g)			0.132	
Amount of stearic acid (g)	4.17		0.14	
Density (g/cm ³)	4.55	1.17	1.19	4.00
Torque (N.m)*	3.98 ± 0.20	4.04 ± 0.04	4.20 ± 0.06	3.50 ± 0.17

The main material was the PZT which was first coated with stearic acid and further kneaded with LDPE using a high-shear mixer (HAAKE PolyLab Mixer, Rheomix 600, Thermo Scientific). The fugitive suspension was a MCC or CB based material. The solid content of the suspensions was adjusted in order to obtain nearly the same torque (viscosity). After kneading, these mixtures were placed in an oven at 130°C for 1 h and afterwards uniaxially pressed (OPUS, Römheld) into a cylinder shaped feedrod (diameter (D) = 24 mm, length (L) = 45 mm). The cylinders were cut on their longitudinal axis into two halves and assembled as shown in Figure 2.

2.2 Co-extrusion investigations and wall slip analyses

The co-extrusion investigations were carried out using one bore of the capillary rheometer (RH7-2, Malvern) following the parameters described in Table 3, at a temperature of 120 °C, based on the crystalline melting point of the LDPE. A 1 mm-diameter die was used so that the extrudate was 24 times smaller than the initial preform. Lengths of 18 cm of each of the co-extruded materials were collected and the area of the cross-section formed by PZT was measured by light microscopy image considering the number of pixels of the lighter area (PZT) using an image analysis software (Gatan Digital Micrograph).

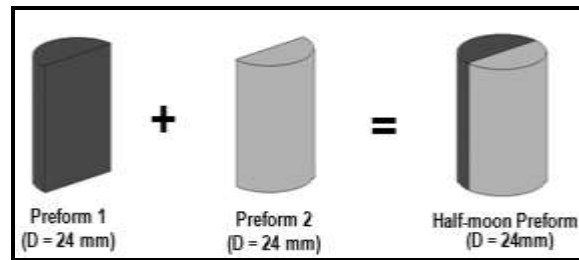


Figure 2. Schematic representation of the preform assembling.

Table 3. Parameters used in the co-extrusion of the PZT half-moon filaments and in the wall slip analyses.

Parameters	Co-extrusion	Wall slip analyses	
		Left bore	Right bore
Shear rate (s ⁻¹)	20	100 – 300 – 500 – 700 – 900	
Half cone angle of the die (°)	60	90	
Diameter / length of the die (mm)	1.00 / 16.00 = 32	0.50 / 8.00 = 32	0.50 / 0.25
		1.00 / 16.00 = 32	1.00 / 0.25
		1.50 / 24.00 = 32	1.50 / 0.25
Pressure sensor (MPa)	350	350	100

In the left bore of the capillary rheometer, the different dies with the same L/D ratio were placed following the description in Table 3. A higher pressure sensor was used in this bore due to the capillary of the die that generates a higher pressure than in the zero die (same diameter but without capillary) placed in the right bore. The wall slip characterisations were carried out for the suspensions described in Table 2. For each suspension, three batches (one for each die diameter) were necessary to carry out the investigations. The capillary rheometer was set using the parameters shown in the Table 3 at a temperature of 120°C.

The raw data obtained from the capillary rheometer were analysed regarding the measured pressure. During the extrusion, points for the pressure drop curve were collected when the equilibrium was achieved. The stabilized pressure drop was measured after a quite long transient zone, related to the reorganization of the powder networks in the die [26]. Three different dies were used in order to apply the Mooney's method. When the capillary diameter increases and consequently its length (to keep the same ratio L/D), the drop pressure necessary to force the material through the capillary increases as well. The pressure drop increased for all suspensions tested, since the flow rate (Q) increases with the capillary diameter, when a shear rate is fixed. The pressure drop increased with the solid content of the feedstock as well. The influence of the entrance effect [27] was measured by the pressure drop on the zero die. During the flow of a material through an orifice without a capillary, all the pressure measured is due to turbulent flow, mass acceleration and viscoelasticity (die swell) effects which happen when the material is forced through the capillary of the die [28]. A capillary rheometer uses the pressure drop to calculate the viscosities so the entrance effect should not be taken into account by the application of Bagley's correction [27]. However, as the aim of this study was a successful co-extrusion, the

materials should have the same rheological behaviour at all and not only the same viscosities. The entrance effect was not diminished from the total pressure drop, as Bagley has proposed. The Rabinowitch correction [28] is required if non-Newtonian substances are tested. Since the material used was a polymer-ceramic system, the Rabinowitch correction was applied on the raw pressure data. To carry on the wall slip analyses, the suspension was considered a homogeneous medium.

3. RESULTS AND DISCUSSION

To verify the influence of the wall slip effect on coextruded structures, the same feedstock of 41 vol. % of MCC was used in both halves of the half-moon structure, just adding a small amount of dye to one of them in order to allow the visualization of the interface. As a result, the successful maintenance of the geometry was achieved after the reduction of 24 times in diameter, proving the effectiveness of the co-extrusion process when both materials exhibit similar rheological behaviour. Afterwards, preforms were assembled being one half a suspension of 58 vol. % PZT and the other half 41 vol. % MCC or 25 vol. % CB. The results of the measurements of the PZT area are shown in Figure 3. From **¡Error! No se encuentra el origen de la referencia.** it can be seen that the fugitive suspensions have almost the same density and both of them exhibited a higher torque value when compared with PZT. However, the flowing behaviour of the auxiliary materials and the PZT was exactly the opposite for the two co-extrusions investigations. The CB mixture exhibited higher torque (viscosity) when compared with the PZT; however, the PZT suspension started flowing at first. The CB curves were the closest and the PZT the most altered ones, what led to the conclusion that the PZT mixture had the higher wall slip effect. On the other hand, during the co-extrusion of MCC + PZT (58vol.%) the conditions were the same, but surprisingly, the MCC started flowing at first. So, there was another parameter influencing the co-extrusion in the capillary rheometer, proving that the matching between the torques (viscosities) of the materials was not enough to reach a successful co-extrusion of a complex cross-section shape. When the cross-sections of the preforms assembled to co-extrude hollow fibre and half-moon filaments are compared (Figure 4), it is noted that the interaction between the materials and between the materials and the wall of the capillary is different. For the hollow fibre geometry, there is a boundary between the materials A and B when a force is applied by a piston in a capillary flow, for example, a relative velocity can appear due to different wall slip velocities for material A and B. On the other hand, only one material (A) is in contact with the wall of the capillary. So, for this geometry the matching of the viscosity of materials A and B could influence more the co-extrusion process than the wall slip effect, achieving the co-extrusion of this preform [23]. Thus, if the materials have nearly the same viscosity and the velocity of the piston is low, the co-extrusion could be successful [10]. On the other hand, when half-moon geometry is used, the same boundary between materials A and B exists, but there are two materials in contact with the wall. Considering that, it was assumed that to have a successful reduction of the diameter using a half-moon preform, the wall slip velocity should be measured at the shear rate in which the viscosities are matching.

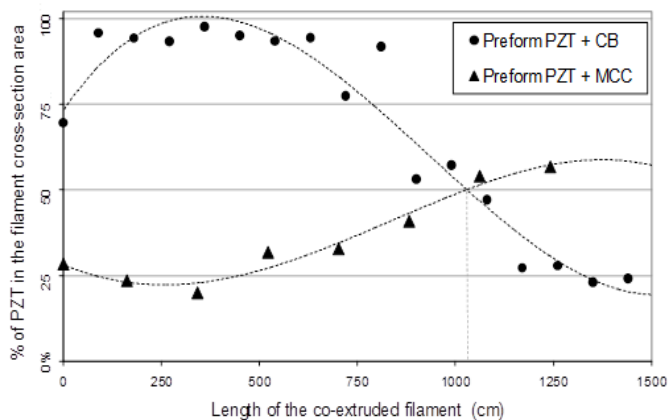


Figure 3. Comparison between PZT + CB and PZT + MCC preform co-extrusions.

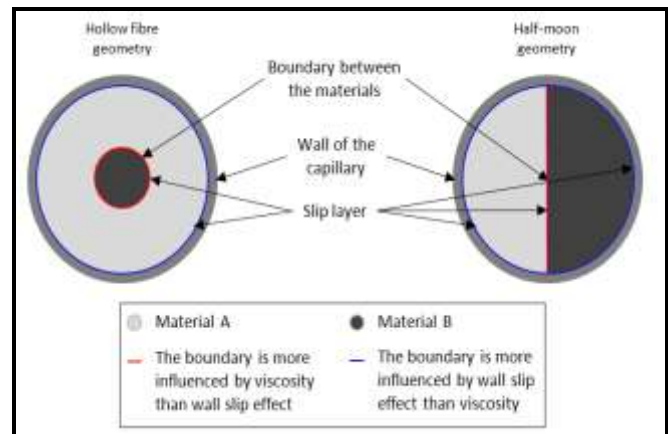


Figure 4. Hypothesis for co-extrusion process.

In view of the results of the investigated co-extrusions, it was assumed that there was another parameter to be considered in addition to the viscosity. Mooney's curves were plotted for the analysed materials (apparent shear rate γ_{app} versus the reciprocal of the die diameter ($1/D$) for a given shear stress at the wall, τ_w . The PZT and MCC mixtures resulted in curves with a correlation factor higher than 0.99, on the other hand, the curves for the CB did not generate reliable correlation factors. The wall slip velocities and the true shear rates were obtained and the slope of the curves increased with the solid content, indicating that the wall slip effect increases as well. However, when these slip velocities and flow rate were plotted in the same graphic, the v_{slip} was found greater than the extruded velocity, what is clearly an unreasonable physical situation in a pressure driven flow. Jastrzebski [29] found empirically that the apparent slip velocity also appears to be affected by the diameter of the capillary tube in addition to the wall shear stress, such that:

$$f(\tau_w) = \frac{\beta}{D} \tau_w \quad (\text{Equation 7})$$

where $\beta = \alpha/D$ is the corrected/modified slip coefficient. Eq. 4 may be rewritten as:

$$\frac{32Q}{\pi D^3} = \frac{4}{\tau_w^3} \int_0^{\tau_w} \tau^2 \gamma d\tau + (8\beta\tau_w) \frac{1}{D^2} \quad (\text{Equation 8})$$

Thus, a plot of the apparent shear rate against $1/D^2$ should produce a straight line for a given wall stress and from the slope ($8\beta\tau_w$) the wall slip velocity can be calculated [29]. The Jastrzebski curves were plotted using $1/D^2$ instead of $1/D$ proposed by Mooney. The values for the wall slip velocities obtained by Jastrzebski can be seen in the Figure 5a.

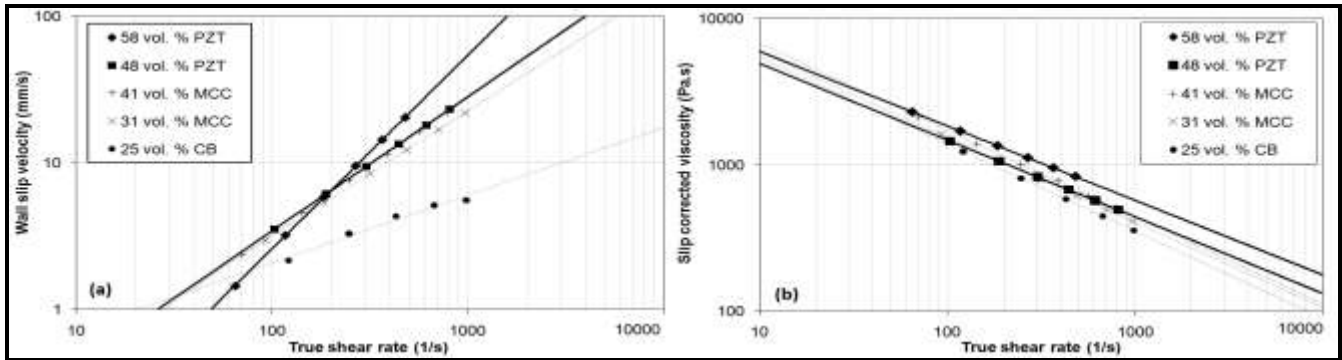


Figure 5. Wall slip analyses. (a) and (b): wall slip velocity and slip corrected viscosity, respectively, as a function of the true shear rate.

The correlation between the slip effect and the results from half-moon co-extrusions was achieved. Figure 5a shows that between 20 and 100^s, referent to the true shear rates, the MCC suspension exhibited the highest wall slip velocity, while the CB the lowest one and the PZT velocity was placed between them. Thus, it might explain the opposite inclination for the flow to start, exhibited when the PZT started flowing before the CB, during the co-extrusion of the half-moon CB/PZT preform and when the MCC did, when the MCC/PZT preform was used (Figure 3). The corrected viscosity can be found when the true shear rate obtained from the wall slip analyses is divided by the correspondent shear stress used to calculate it [19]. In contrast to conventional thermoplastics, the viscosity data without the slip phenomena taken into account depend on the diameter of a capillary die: the larger the diameter, the larger the viscosity (Figure 5b) [20].

Taking into account that in concentrated suspensions the solid content influences the intensity of the wall slip effect, a different behaviour was exhibited by the PZT feedstock with 58 vol. % of solid, exhibiting the most singular slope. The cause might be a high solid content which could have exceeded the critical value, as observed for Gorislavets *et al.* [22]. Hence, to verify the influence of the solid content, a PZT suspension with a lower solid content (48 vol. % of PZT) was prepared. The torque obtained for this composition was around 3.5 N.m (Table 2), which was lower than the standard considered for adjusting the solid content of the previous suspensions. The slope of the 48 vol. % PZT curve showed a better agreement with the MCC curves.

From the power trend lines of the graphics “wall slip velocity vs. true shear rate” and “slip corrected viscosity vs. true shear rate”, the exact shear rate in which the materials would have the same velocity or viscosity were calculated. The results are shown in Table 4. The apparent shear rate for setting on the capillary rheometer

during co-extrusion was calculated and each case was analysed individually. A successful co-extrusion regarding the capability of the preform to maintain the geometric shape was expected when the wall slip velocities and the slip corrected viscosities were matching for both suspensions at the same time for the same shear rate. So, for 48 vol. % PZT and 41 vol. % MCC the intersection points were obtained and the co-extrusion when only the wall slip velocities were matching (at 12.223 per second, as the shear rate) was not done, since this high value and the almost parallel curves, could be interpreted as if they showed comparable slip behaviours. So, considering the same wall slip velocities and slip corrected viscosities for the preforms, the co-extrusion was done at a shear rate of 965 s⁻¹. The possibility of a turbulent flow was taken into account due to high shear rates used in the processing [28], but the preform of 48 vol. % of PZT and 41 vol. % of MCC could maintain its geometry during all co-extrusion process. The successful co-extruded filaments obtained are shown in Figure 6.

Table 4 Hypothesis about the co-extrusion behaviours.

Vol. % PZT	Vol. % MCC	Shear rate (1/s)	Comparison between viscosities	Comparison between wall slip velocities	Predicted behaviour
58	31	149	$\eta_{PZT} > \eta_{MCC}$	$V_{slip, PZT} = V_{slip, MCC}$	MCC should start flowing before PZT.
		-1	* Shear rate physically not reasonable.		
58	41	180	$\eta_{PZT} > \eta_{MCC}$	$V_{slip, PZT} = V_{slip, MCC}$	MCC should start flowing before PZT for both cases.
		39	$\eta_{PZT} = \eta_{MCC}$	$V_{slip, PZT} < V_{slip, MCC}$	
48	31	28	$\eta_{PZT} < \eta_{MCC}$	$V_{slip, PZT} = V_{slip, MCC}$	PZT should start flowing before MCC for both cases, but it has not happened.
		202	$\eta_{PZT} = \eta_{MCC}$	$V_{slip, PZT} > V_{slip, MCC}$	
48	41	12.223	* Not tested due to the fact that this shear rate is too high for the equipment.		The co-extrusion was successful.
		965	$\eta_{PZT} = \eta_{MCC}$	$V_{slip, PZT} = V_{slip, MCC}$	



Figure 6. Photos of successfully co-extruded half-moon filaments.

4. CONCLUSIONS

To investigate the influence of wall slip behaviour of different materials during MFCX process a so called half-moon structure was used. Due to this setup, an interface between two materials as well as the interaction between the two feedstocks and the die wall (so called wall slip effect) can be analysed by image analysis. In this study three different polymer compounds were used. The viscosity and wall slip behaviour of a lead zirconate titanate, carbon black and micro crystalline cellulose based polyethylene thermoplastic compound was studied in detail. All feedstocks used in this work were able to be characterised regarding the wall slip effect applying Mooney's method and Jastrzebski correction. Neither interface nor internal structure retained after co-extrusion of the half-moon structures using the processing area of the cross over point of the feedstocks viscosity. Only for the pure MCC half-moon structure (one with small amount of dye) well defined interface and stable internal shape structure occurred. Only by using the cross over point of the slip corrected viscosity and a similar wall slip behaviour of the two compounds (similar solid content), co-extrusion process of the half-moon structure was successful.

REFERENCES

1. P. and J. Curie, Comptes Rendus, 1880, 91, 294.
2. Hankel, Abh. Sächs., 1881, 12, 457.

3. L. J. Nelson, "Smart piezoelectric fibre composites"; *Mater. Sci. Technol.*, 2002, 18, 1245–1256.
4. J. J. Benbow and J. Bridgwater, "Paste Flow and Extrusion", Oxford Univ. Press Inc, New York, 1993.
5. M. Rides and C. Allen, "Extensional flow properties of polymer melts using converging flow methods", National Physical Lab., Teddington, United Kingdom, 1999.
6. Y. Zhou, "Optimization of Fiber Shapes in Biocomposites", Dissertation submitted to the Graduate School of the University of Notre Dame, Indiana, USA, 2005.
7. R. B. Cass, "Fabrication of continuous ceramic fibre by the viscous suspension spinning process", *Am. Ceram. Soc. Bull.*, 1991, 70, 424-429.
8. J. Yue *et al.* "The influence of sintering conditions on the dielectric and piezoelectric properties of PbZrTiO–PbMgNbO ceramic tubes", *J. of Alloys and Compounds*, 2009, 470, 465-469.
9. C. Kaya, E. G. Butler, M. H. Lewis, "Co-extrusion of Al₂O₃/ZrO₂ bi-phase high temperature ceramics with fine scale aligned microstructures", *J. of European Ceramic Soc.*, 2003, 23, 935–942.
10. M. R. Ismael *et al.*, "Effects of rheology on the interface of Pb(Zr,Ti)O₃ monofilament composites obtained by co-extrusion", *Journal of the European Ceramic Society*, 2009, 29, 3015–3021.
11. J. F. Fernandez *et al.*, "Hollow piezoelectric compounds", *Sensors and act. A*, 1996, 51, 183-192.
12. D. Brei, B. Cannon Jr., "Piezoelectric hollow active composites", *Comp. science and techn.*, 2004, 64, 245-261.
13. M. Takase, S. Kihara, K. Funatsu, "Three-dimensional viscoelastic numerical analysis of the encapsulation phenomena in coextrusion", *Rheologica Acta*, 1998, 37, 624–634.
14. C. V. Hoy *et al.*, "Microfabrication of Ceramics by Co-extrusion", *Journal of American Ceramic Society*, 1998, 81, 152–158.
15. C. B. Yoon *et al.*, "Transverse 1-3 piezoelectric ceramic/polymer composite with multi-layered PZT ceramic blocks", *Sensor. Actuat. A: Phys.*, 2007, 134, 480–485.
16. A. T. Crumm *et al.*, "Micro-configured piezoelectric artificial materials for hydrophones", *J. Mater. Sci.*, 2007, 42, 3944–3950.
17. J. Powell and S. Blackburn, "The unification of paste rheologies for the co-extrusion of solid oxide fuel cells", *Journal of the European Ceramic Society*, 2009, 29, 893-897.
18. J. Dooley and L. Rudolph, "Viscous and elastic effects in polymer coextrusion", *J. Plast. Film Sheet*, 2003, 19, 111–122.
19. N. Minagawa and J. L. White, "Co-extrusion of unfilled and TiO₂-filled polyethylene: influence of viscosity and die cross-section on interface shape", *Polym. Eng. Sci.*, 1975, 15, 825–830.
20. T. H. Kwon and S. Y. Ahn, "Slip characterization of powder/binder mixtures and its significance in the filling process analysis of powder injection moulding". *Powder Technology*, 1995, 85, 45-55.
21. M. Mooney, "Explicit formulas for slip and fluidity", *Journal of rheology*, 1931, 210-222
22. V. M. Gorislavets and A. A. Dunets, "Rheological properties of concentrated suspensions in the presence of the wall effect". *J. of Engineering Physics and Thermophysics*, 1975, 29, 1008-1014.
23. M. R. Ismael, V. L. Bueno, F. Clemens, T. Graule and M. J. Hoffmann, "Process chain development for the microfabrication of solid and hollow ferroelectric fibers by co-extrusion", in preparation.
24. Ismael, M.R., Clemens, F., *et al.*, Processing, microstructure and electromechanical properties of Pb(Zr, Ti)O₃ fibers obtained by thermoplastic co-extrusion, *IEEE International Symposium on the Application of Ferroelectrics*, (2009).doi: 10.1109/ISAF.2009.5307603
25. J. Heiber, F. Clemens, T. Graule and D. Hülsenberg, "Thermoplastic extrusion to highly-loaded thin green fibres containing Pb(ZrTi)O₃", *Adv. Eng. Mater.*, 2005, 7, 404–408.
26. B. Lanteri *et al.* "Rheological behavior of a polymer-ceramic blend used for injection moulding", *Journal of materials science*, 1996, 31, 1751-1760.
27. E. B. Bagley, "End Corrections in the Capillary Flow of Polyethylene". *Journal of Applied Physics*, 1957, 28, 624-628.
28. S. Q. Wang. "Molecular Transitions and Dynamics at Polymer/Wall Interfaces: Origins of Flow Instabilities and Wall Slip". In: Granick (Ed.), "Polymers in Confined Environments", *Advances in Polymer Science*, 1999, 138, 227-275.
29. D. Z. Jastrzebski, "Entrance effects and wall effects in an extrusion rheometer during the flow of concentrated suspensions". *Experimental Technique*, 1967, 6, 445-454.